Bioorganic & Medicinal Chemistry Letters 19 (2009) 2299–2304

Contents lists available at ScienceDirect

Bioorganic & Medicinal Chemistry Letters

journal homepage: www.elsevier.com/locate/bmcl

Inhibitors of potassium channels $K_V1.3$ and IK-1 as immunosuppressants

Stefano Pegoraro [a], Martin Lang [a], Tobias Dreker [a], Jürgen Kraus [a], Svetlana Hamm [a], Cathal Meere [a], Juliane Feurle [a], Stefan Tasler [a,*], Sylvia Prütting [b], Zerrin Kuras [b], Violeta Visan [b], Stephan Grissmer [b,*]

[a] 4SC AG, Am Klopferspitz 19a, 82152 Planegg-Martinsried, Germany
[b] Institute of Applied Physiology, University of Ulm, Albert-Einstein-Allee 11, 89081 Ulm, Germany

ARTICLE INFO

Article history:
Received 23 December 2008
Revised 19 February 2009
Accepted 20 February 2009
Available online 25 February 2009

Keywords:
Potassium channel
IK-1
$K_V1.3$
Homology model
vHTS
Autoimmune diseases

ABSTRACT

New structural classes of $K_V1.3$ and IK-1 ion channel blockers have been identified based on a virtual high throughput screening approach using a homology model of KcsA. These compounds display inhibitory effects on T-cell and/or keratinocyte proliferation and immunosuppressant activity within a DTH animal model.

In human T-cells the Ca^{2+}-dependent potassium channel IK-1 ($K_{Ca}3.1$) and the voltage-gated potassium channel $K_V1.3$ have been shown to play a pivotal role during cell proliferation. They are crucial mediators for the repolarization of the cell membrane upon cell stimulation, maintaining an intracellular Ca^{2+} signal decisive for the proliferation process. IK-1 and $K_V1.3$ channels display different distributions among certain T-cell subsets, which additionally varies depending on the activation state: Upon activation, IK-1 is predominant in naïve and central memory T-cells and $K_V1.3$ in effector memory T-cells (T_{EM} cells).[1] Blockade of these channels is linked to inhibition of proliferation, which was proven using small molecule specific inhibitors such as TRAM-34[2] for IK-1 and PAP-1[3] for $K_V1.3$ (Fig. 1).[1] Consequently, both channels are considered as potential targets for modulating immune response, which would be desirable for treating autoimmune diseases like multiple sclerosis, rheumatoid arthritis, diabetes type 1 and the skin disease psoriasis,[1,4] in which IK-1 might also play a role in the proliferation of keratinocytes (HaCaT cell line).[5]

High throughput screening for ion channel modulators is hampered by technical difficulties (even though decreasingly): Either the screening method provides data of good quality and information content but does not allow for a high throughput (patch clamp assay), or a loss of reproducibility, quality or functional information has to be accepted as a price for higher throughput.[6] Consequently, a combination of a rational pre-selection of screening compounds along with a patch clamp assay was expected to circumvent the throughput problems without sacrificing the high quality of data points. For such a purpose, virtual high throughput screening (vHTS) composed of a docking experiment using 4SCan® technology[7] was envisaged. Based on the data published for disease relevance of these potassium channels at that time,[4,8] primary focus was laid on the discovery of potent small molecule inhibitors for $K_V1.3$. Back then, a crystal structure of a mammalian potassium channel was not available—this changed not before 2005[9]—thus initial modeling was based on a homology model for $K_V1.3$ assembled from the crystal structure of the bacterial KcsA channel.[10] The inner vestibule (i.e., the internal cavity just below the K^+-selectivity pore) was selected as binding pocket for potential inhibitors, as this binding site was identified as such for TRAM-34 in IK-1 and is assumed to be addressed by PAP-1 in $K_V1.3$ as well.[1,11] Within this region, both $K_V1.3$ and IK-1 display around 45% homology with KcsA. The $K_V1.3$ model generated was applied to the evaluation of a data base of 3.3 Mio virtual and commercially available compounds. Out of the list of best 500 compounds, a selection was made combining a certain structural diversity with good docking scores within the binding pocket. Current blocking activity on $K_V1.3$ was determined for 37 compounds using patch clamp technology,[12,13] for which a hit rate of around 11% was found when defined as $IC_{50}(K_V1.3)$ below 10 μM. A few structurally significantly different intriguing compounds were identified, among which dihydrophenanthridine **1** displayed already good inhibitory

* Corresponding authors. Tel.: +49 89 7007630; fax: +49 89 700763 29 (S.T.); fax: +49 731 5023260 (S.G.).
E-mail addresses: stefan.tasler@4sc.com (S. Tasler), stephan.grissmer@uni-ulm.de (S. Grissmer).

0960-894X/$ - see front matter © 2009 Elsevier Ltd. All rights reserved.
doi:10.1016/j.bmcl.2009.02.077

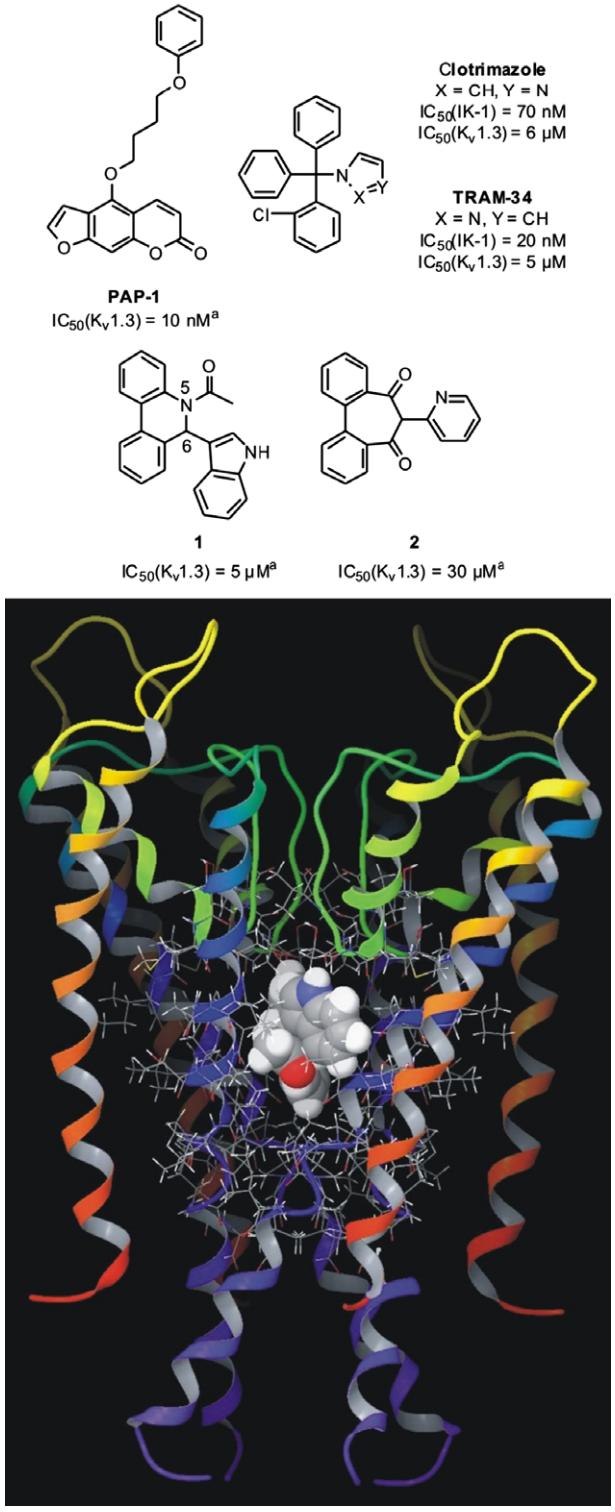

Figure 1. Reference compounds for $K_V1.3$ and IK-1 inhibition, hit molecule **1** and analog **2** identified based on vHTS; compound **1** is shown within the inner vestibule of the $K_V1.3$ homology model (closed state of the channel); [a]values determined in-house.

potential on $K_V1.3$ (Fig. 1). In addition, another bridged biaryl, the dibenzocycloheptanedione derivative **2**, showed some moderate activity as well, already indicating a possible direction for structural variations around the hit molecule **1**.

A quick approach for substitutional variations at N5 and C6 of the 5,6-dihydrophenanthridine scaffold was established, including activation of the imine structure in phenanthridine (**3**) with acyl chlorides to give an intermediary imminium ion enabling in situ nucleophilic attack at C6 with indoles or pyrroles as well as with Grignard reagents (Scheme 1).[14] An inverse strategy was realized for the synthesis of derivative **6**, for which the phenanthridine (**3**) was first treated with a Grignard reagent, followed by N-acylation.[15] Oxalylic acid derivative of entry 6 (Table 1) was attained by saponification of the corresponding ester [entry 7; LiOH, MeOH/H_2O (3:1), 90 °C, 2 h, 48%].

Based on the promising results for $K_V1.3$ blockade (Table 1, discussion below), further structural variations were scheduled, including alterations of the bridging unit of the biaryl core towards the second molecule depicted in Figure 1, dibenzocycloheptanedione **2**. Phenanthridinone derivatives were simply N-alkylated in DMF starting with phenanthridin-6(5*H*)-one (Table 2, entry 19) using the corresponding alkyl bromides (KOH, K_2CO_3, cat. TBAB, 110 °C, 1 h) (e.g., entry 20, exemplarily shown in Table 2). *N*-acyl derivatives of phenanthridinone—as closer analogs for the series depicted in Table 1—proved to be rather unstable (isomerization and/or decomposition)[16] and were consequently not suitable for evaluation of biological effects. Extending the bridging unit from a six-membered to a seven-membered ring required a multi-step synthesis of 5*H*-dibenzo[*b*,*d*]azepin-7(6*H*)-ones **9** (Table 2, entries 21–25) (Scheme 2). The sequence involved an intramolecular Friedel–Crafts acylation in **8** as crucial step.[17]

Due to the already decent level of activity on $K_V1.3$, the screening concentration for phenanthridine derivatives within the patch clamp assay was chosen to be 2 μM (Table 1), as compared to 20 μM for the other de-novo scaffold variations in Table 2. Out of the numerous derivatives synthesized for the former class of compounds, a selection is given in Table 1. Starting with the initial hit molecule **1**, the *N*-acetyl unit was replaced by other aliphatic *N*-acyl variants (entries 2–5), but a clear SAR was not deducible. A cyclobutyl residue at the *N*-carbonyl unit (entry 4) gave rise to a comparable IC_{50} value as observed for the methyl residue in the parent compound **1**, 2-propyl was worse, 2-pentyl better (entries 2 and 3 vs entry 1). From entries 5 and 8 it can be concluded, that further aliphatic extension for an attachment of a cyclic residue (cyclopentyl or phenyl, respectively) is not tolerated.

Oxalylic derivatives (entries 6 and 7) resulted in quite decent activities on $K_V1.3$ with IC_{50} values around 1–3 μM. Direct aromatic substitution at the *N*-carbonyl linker bears some potential

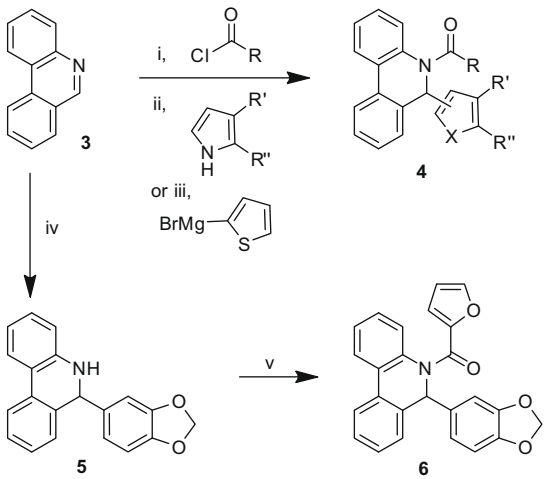

Scheme 1. Reagents and conditions: (i) toluene or DMF (THF, if second step is Grignard reaction), rt, 1 h; (ii) NEt_3 or DIEA, rt, 20 h; 5–70%; (iii) rt, 20 h; 29–42%; (iv) benzo[*d*][1,3]dioxol-5-ylmagnesium bromide, THF, 65 °C, 7 h, 50%; (v) 2-furoyl chloride, THF, NEt_3, rt, 2 h, 19%; reactions performed in inert atmosphere.

Table 1
$K_V1.3$ activities for selected phenanthridine derivatives

	Entry	R		$IC_{50}(K_V1.3)$ [μM] (inhib. @ 2 μM)
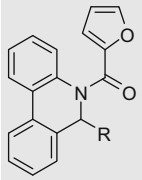	1[a]			5.0
	2			7.4
	3	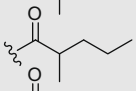		1.9
	4			4.2
	5	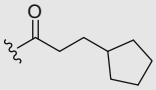		– (11%)
	6	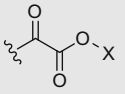	X = H	– (41%)
	7		Me	1.4
	8	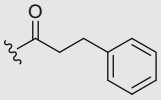		– (15%)
	9	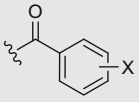	X = 2-OMe	– (51%)
	10		3-OMe	– (30%)
	11		4-OMe	– (13%)
	12	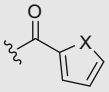	X = S	– (43%)
	13		O	1.5
	14	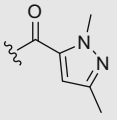		0.71
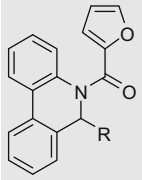	15			– (15%)
	16	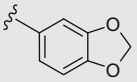		– (8%)
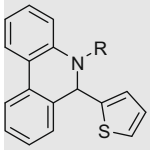	17	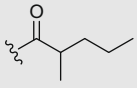		– (59%)
	18	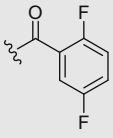		– (27%)

[a] Commercial sources.

for further optimization of $K_V1.3$ blocker capability: incorporation of a 2-anisolyl as well as 2-thienyl or 2-furanyl resulted in IC_{50} values between 1.5 and 3 μM (entries 9, 12 and 13; inhibition of 43% at 2 μM should result in an IC_{50} around 3 μM)—comparable to the 2-pentyl derivative of entry 3—but now offering the possibility for amelioration of activity by tuning the heterocyclic group or further aromatic substituents. Keeping a five-membered heterocycle in place, the dimethylpyrazole derivative gave rise to a sub-micromolar activity (entry 14) and thus represents an excellent lead for further optimizations. A substitution of the 3-indolyl moiety at C6 of the dihydrophenanthridine by 2-pyrrolyl or benzo[*d*][1,3]dioxol-5-yl was detrimental to activity (entries 15 and 16 vs entry 13), whereas the 2-thienyl group at C6 resulted in virtually identical activity for the *N*-(2-methylpentanoyl) derivative with an IC_{50} somewhat below 2 μM (entry 17 vs entry 3).

Variations of the bridging unit started with the elimination of the aromatic C6-substituent, now utilizing a phenanthridin-6(5*H*)-one scaffold. Besides the parent scaffold, one derivative is

Table 2
$K_V1.3$ activities for differently bridged biaryl derivatives

	Entry	R		$IC_{50}(K_V1.3)$ [μM] (inhib. @ 2 μM)
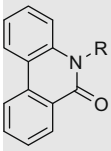	19[a]	H		— (12%)
	20	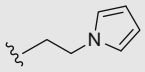		— (57%)
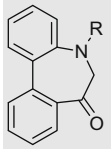	21[a]	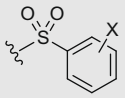	X = 4-Me	5.8
	22		4-NO_2	>10
	23		4-Cl	6.1
	24		3-Cl	3.6
	25	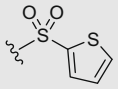		13
	26	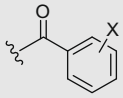	X = 4-Me	4.0
	27		3-Cl	3.4

[a] Commercial sources.

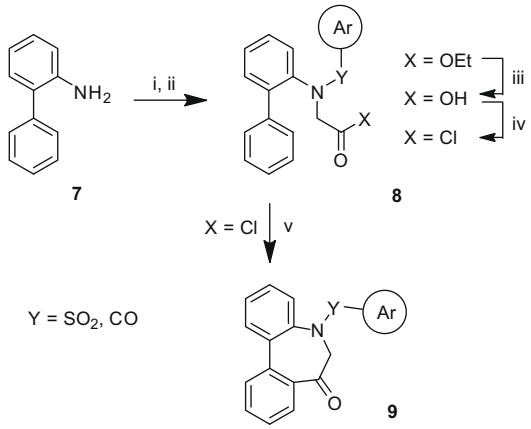

Scheme 2. Reagents and conditions: Variant A: (i) $ArSO_2Cl$, pyridine, 140 °C, 30 min, quant.; (ii) ethyl bromoacetate, Na_2CO_3, toluene, 110 °C, 4 h, 15–30%; (iii) NaOH, MeOH/H_2O (3:1), 30 °C, 4 h, quant.; (iv) $SOCl_2$, 75 °C, 1 h; (v) $AlCl_3$, $CHCl_3$, −78 °C to rt, 2 h, 5–50% over two steps. Variant B: (i) ethyl bromoacetate, Na_2CO_3, toluene, 110 °C, 4 h, 14%; (ii) ArCOCl, pyridine, 125 °C, 3 h; (iii) NaOH, MeOH/H_2O (3:1), 70 °C, 4 h; (iv) $SOCl_2$, rt, 2 h; (v) $AlCl_3$, $CHCl_3$, −78 °C to rt, 20 h, 16–25% over four steps.

shown exemplarily in Table 2 (entry 20), which reflects the general loss of activity on $K_V1.3$ (best value: 57% current blocking @ 20 μM). Extension of the bridging unit by an additional methylene group was evaluated initially for compound entry 21, in which the carbonyl attachment to the endocyclic nitrogen as present in derivatives of Table 1 was simultaneously replaced by sulfonyl simply based on commercial availability of such a compound. As a moderate activity on the $K_V1.3$ channel was identified, further derivatives were synthesized either as sulfonamides (entries 22–25) or now also as carboxamides (entries 26 and 27) (only selected derivatives shown in Table 2). Best IC_{50} values were determined between 3.4 and 6.1 μM with carboxamides and sulfonamides displaying virtually identical inhibition (entries 21 and 24 vs entries 26 and 27, respectively).

With proliferation of T-cells being mediated by either $K_V1.3$ or IK-1 depending on the T-cell subtype (vide supra) and a sequence homology for the inner vestibule of the two channels of around 55%, selected derivatives out of Tables 1 and 2 were cross-evaluated on the latter ion channel (patch clamp assay).[18] As can be seen in Table 3, phenanthridines and phenanthridinones displayed virtually no activity on IK-1 (entries 3, 13, 14 and 20), whereas compounds of the 5*H*-dibenzo[*b*,*d*]azepin-7(6*H*)-one series (entries 21, 23 and 25–27) possessed some potency on IK-1. Independent from the nature of the substituent at the sulfon moiety (entries 21, 23 and 25), IC_{50}(IK-1) values were identified around 2 μM. For corresponding carboxamide derivatives, the 4-Me variant lost significantly inhibitory potency at IK-1 (entry 26 vs entry 21, 16 μM vs 2.1 μM), the 3-chlorinated variant, however, displayed good activity on this potassium channel comparable to the 4-chlorophenylsulfonamide of entry 23, IC_{50} values were determined to be around 1.3 μM.

Upon identification of effective potassium channel blockers—entry 14 for $K_V1.3$, entries 21, 23, 25 and 27 for IK-1—their effect on the proliferation of the T_{EM} cell fraction of PBMCs was investigated (Table 4). For this purpose, PBMCs were stimulated using anti-CD3 antibody,[19] upon which neither a potent $K_V1.3$ blocker (PAP-1) nor an IK-1 blocker (TRAM-34) alone were able to inhibit proliferation significantly up to a concentration of above 20 μM. With a background of an IK-1 blocker supplied at 5 μM, dose–response curves were attained for the $K_V1.3$ blocker in question, indicating that proliferation of T_{EM} cells according to this protocol is mediated by two components, an IK-1 and a $K_V1.3$ based mechanism. Within this setup, PAP-1 was determined to have an EC_{50} of 430 nM (TRAM-34 background), with a significant deviation in dependence on the PBMC donor (±350 nM). For the phenanthridine of entry 14, an EC_{50} of 12.5 μM was identified (TRAM-34 background), which represents a slightly improved factor towards the EC_{50} of PAP-1 (EC_{50} ratio ~30) as compared to the factor present for activity at the $K_V1.3$ (factor ~70). However, the activity of this compound was not significantly altered by the presence of an IK-1 blocker: EC_{50} = 15 vs 12.5 μM. As a virtual inactivity at the IK-1 (12% current blocking at 20 μM) cannot account for this finding, influences of this compound on calcium signaling in anti-CD3 stimulated PBMCs was investigated.[20] These experiments revealed a dose dependent reduction of the thapsigargin-induced increase in the intracellular calcium concentration unlike that of potassium channel blockers tested (PAP-1, TRAM-34), thus indicating an additional interference with the calcium signaling, ultimately adding another potential effect on T-cell proliferation.

An identical concept as pursued for $K_V1.3$ blockers was realized for the evaluation of entries 21 and 23 as IK-1 inhibitors. Thus,

Table 3
Activities on IK-1 and HaCaT

Compound entry	$IC_{50}(K_V1.3)$ [μM]	IC_{50}(IK-1) [μM]	EC_{50}(HaCaT) [μM]
3	1.9	No effect	14
13	1.5	No effect	17% inhib. at 25 μM
14	0.71	12% inhib. at 20 μM	nd
20	57% inhib. at 20 μM	No effect	2.3
21	5.8	2.1	8.4
23	6.1	1.4	n.d.
25	13	2.4	n.d.
26	4.0	16	n.d.
27	3.4	1.3	n.d.
PAP-1	0.01	10[a]	n.d.
TRAM-34	5.0[b]	0.02[b]	40
Clotrimazole	6.0[b]	0.07[b]	15

n.d. = not determined.
[a] Data taken from Ref. 26.
[b] Data taken from Ref. 2.

Table 4
Inhibition of anti-CD3 stimulated PBMC proliferation; values are means of $n \geqslant 2$ individual experiments

$K_V1.3$ blocker	IK-1 blocker	EC_{50} of	EC_{50} [μM]
—	TRAM-34	TRAM-34	No effect
—	Entry 21	Entry 21	No effect
—	Entry 23	Entry 23	No effect
PAP-1	—	PAP-1	~25
PAP-1	TRAM-34 [5 μM]	PAP-1	0.43
PAP-1	Entry 21 [5μM]	PAP-1	0.4
PAP-1	Entry 23 [5 μM]	PAP-1	1.2
PAP-1	Entry 23 [16.7 μM]	PAP-1	0.5
Entry 14	—	Entry 14	~15
Entry 14	TRAM-34 [5 μM]	Entry 14	12.5
PAP-1 [5 μM]	TRAM-34	TRAM-34	0.025
PAP-1 [5 μM]	Entry 21	Entry 21	2.5
PAP-1 [5 μM]	Entry 23	Entry 23	8.0

dose–response curves for these compounds were measured with a 5 μM background of PAP-1 present, which proved their activity as IK-1 blockers. Their EC_{50} values of 2.5 and 8.0 μM were found to be within the same range compared to TRAM-34 as were IC_{50} patch clamp data for these compounds (factor 80–320). A final prove of potent IK-1 blockade was achieved by substituting the TRAM-34 background for either one of the compounds of entry 21 and 23 in PAP-1 EC_{50} determinations. With a background of IK-1 blocker chosen appropriately high (concn > EC_{50} of the respective compound with 5 μM PAP-1 background), PAP-1 activity was identical for all compounds, EC_{50}s(PAP-1) were determined between 400 and 500 nM (same PBMC donor).

As mentioned above, with regard to targeting psoriasis, IK-1 was discussed to be involved in the proliferation process of keratinocytes,[5] so that inhibition of this potassium channel was proposed to have a potential for the inhibition of proliferation of human HaCaT cells. However, no correlation between inhibition of HaCaT proliferation[21] and IK-1 activity can be deduced from the data shown (Table 3). The best EC_{50} value on these cells was attained for the pyrrolylethyl phenanthridinone derivative of entry 20 with 2.3 μM, which displayed no activity on IK-1. Vice versa, the potent IK-1 inhibitors TRAM-34 and clotrimazole displayed only a weak effect on HaCaT cells with EC_{50} values of 40 and 15 μM, respectively.

A general cytotoxic effect in either assay, inhibition of PBMC or HaCaT proliferation, could be excluded for selected compounds: cell viability was determined on either HaCaT cells or PBMC for compounds of entry 14 and 21 in comparison with clotrimazole. Whereas clotrimazole displayed an LD_{50} of ~40 μM, no cytotoxic effect was measurable for both compounds mentioned up to 50 μM (highest assay concentration). Furthermore, a caspase 3/7 assay was performed for compounds of entries 7, 20 and 21 in order to check for apoptosis induction, which could be excluded in a concentration range up to 30 μM for all three compounds. Finally, clotrimazole, TRAM-34 and the compound of entry 21 were tested for proliferation inhibition on HEK-293, the proliferation of which should be IK-1 independent, only to identify the EC_{50} values to be rather similar. Thus, inhibition of HaCaT proliferation should be neither based on cytotoxic effects and apoptosis nor on IK-1 inhibition—with the latter being in good agreement with the data collection presented (Table 3).

5*H*-Dibenzo[*b*,*d*]azepin-7(6*H*)-one of entry 21 was next selected for a comparison study with clotrimazole for the anti-inflammatory potential in a mouse DTH model (delayed-type hypersensitivity; ear swelling). Generally, mouse T_{EM} cells do not up-regulate $K_V1.3$ expression upon activation and—besides $K_V1.3$ and IK-1—express further members of the $K_V1.x$ family in T-cells. Consequently adjustment of their membrane potential

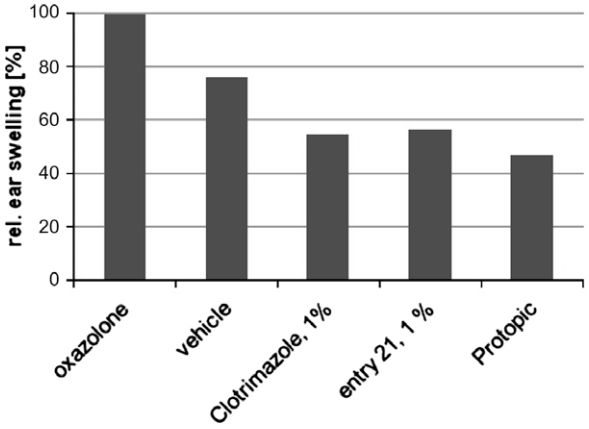

Figure 2. Relative inhibition of ear swelling in a DTH mouse model (oxazolone sensitization/challenge) for clotrimazole and compound of entry 21 (each 1% in ethanol–DMSO 4:1) in comparison with Protopic® (0.1%); values are means of $n = 5$ animals per group.

and eventually proliferation is not dependent on a functional $K_V1.3$ unit.[1] On the other hand, IK-1 mRNA expression was identified in $CD4^+$ T lymphocytes in wild-type mice and its essential role within these cells was proven by IK-1 inhibition using clotrimazole and also in *Kcnn4* knock-out mice.[22,23] Therefore, an anti-inflammatory effect possibly detectable in this mouse model working via inhibition of T-cell proliferation might be mediated by a dominant IK-1 effect of the compounds. Both compounds were administered once topically in ethanol–DMSO as vehicle (compound concentration of 1%) 30 min after challenge (oxazolone) and resulted in comparable reductions of ear swelling of ca. 20 percentage points towards the vehicle treated group (Fig. 2). Protopic® (0.1%) was used as positive control. Its active ingredient interferes with Ca^{2+} signaling in T-cells by binding to calcineurin. As 5*H*-dibenzo[*b*,*d*]azepin-7(6*H*)-one of entry 21 showed an analogous, even though slightly weaker decrease of intracellular calcium levels in thapsigargin-treated T-cells[20] as observed for phenanthridine of entry 14 (vide supra) and unlike that of a potent IK-1 blocker, an additional effect on calcium signaling might explain the similar activity in this DTH model as compared to clotrimazole besides its weaker inhibition of IK-1.

Based on a vHTS approach, two structurally new classes of potassium channel inhibitors have been identified as new leads for further optimization processes.[24] The phenanthridine of entry 14 displayed an IC_{50} of 710 nM for $K_V1.3$ inhibition. Besides several peptidic toxins, only a few small molecules have been reported as sub-micromolar inhibitors of the $K_V1.3$[1,25]—that is mainly PAP-1 and its derivatives,[3,26] PAC derivatives[27] and khellinones[19]—so that this scaffold represents a promising lead for a new effective class of such inhibitors, being non-cytotoxic and not displaying any issues on the hERG channel. Likewise intriguing are the IK-1 blockers of the 5*H*-dibenzo[*b*,*d*]azepin-7(6*H*)-one type, entries 21, 23 and 27, with IC_{50} values of 2.1, 1.4 and 1.3 μM, respectively. The former compound (entry 21) displayed anti-inflammatory potential in a mouse DTH model comparable to clotrimazole. These potassium channel inhibitors were effective inhibitors of T_{EM} cell proliferation in an appropriate assay setup.

Acknowledgements

The authors want to thank Dr. Wael Saeb for synthetic assistance and Drs Andrea Aschenbrenner, Andreas Wuzik, Udo Sinks and Daniel Vitt for scientific input. Funding by the BMBF (BioChance Plus) was highly appreciated.

References and notes

1. Wulff, H.; Zhorov, B. S. *Chem. Rev.* **2008**, *108*, 1744.
2. Wulff, H.; Miller, M. J.; Hänsel, W.; Grissmer, S.; Cahalan, M. D.; Chandy, K. G. *Proc. Natl. Acad. Sci. U.S.A.* **2000**, *97*, 8151.
3. Vennekamp, J.; Wulff, H.; Beeton, C.; Calabresi, P. A.; Grissmer, S.; Hänsel, W.; Chandy, K. G. *Mol. Pharmacol.* **2004**, *65*, 1364.
4. (a) Jensen, B. S.; Strobaek, D.; Olesen, S.-P.; Christophersen, P. *Curr. Drug Targets* **2001**, *2*, 401; (b) Jensen, B. S.; Hertz, M.; Christophersen, P.; Madsen, L. S. *Exp. Opin. Ther. Targets* **2002**, *6*, 623.
5. Koegel, H.; Alzheimer, C. *FASEB J.* **2001**, *15*, 145.
6. (a) Dabrowski, M. A.; Dekermendjian, K.; Lund, P.-E.; Krupp, J. J.; Sinclair, J.; Larsson, O. *CNS Neurol. Disord. Drug Targets* **2008**, *7*, 122; (b) Southan, A.; James, I. F.; Cronk, D. *Drug Discovery World* **2005**, *6*, 17; (c) Xu, J.; Wang, X.; Ensign, B.; Li, M.; Wu, L.; Guia, A.; Xu, J. *Drug Discovery Today* **2001**, *6*, 1278.
7. Seifert, M. H. J.; Wolf, K.; Vitt, D. *Biosilico* **2003**, *1*, 143.
8. (a) Beeton, C.; Wulff, H.; Barbaria, J.; Clot-Faybesse, O.; Pennington, M.; Bernard, D.; Cahalan, M. D.; Chandy, K. G.; Beraud, E. *Proc. Natl. Acad. Sci. U.S.A.* **2001**, *98*, 13942; (b) Wulff, H.; Calabresi, P. A.; Allie, R.; Yun, S.; Pennington, M.; Beeton, C.; Chandy, K. G. *J. Clin. Invest.* **2003**, *111*, 1703.
9. Long, S. B.; Campbell, E. B.; MacKinnon, R. *Science* **2005**, *309*, 897.
10. Zhou, Y.; Morais-Cabral, J. H.; Kaufman, A.; MacKinnon, R. *Nature* **2001**, *414*, 43.
11. Wulff, H.; Gutman, G. A.; Cahalan, M. D.; Chandy, K. G. *J. Biol. Chem.* **2001**, *276*, 32040.
12. For a general description of patch clamp methodology, see: Hamill, O. P.; Marty, A.; Neher, E.; Sakmann, B.; Sigworth, F. J. *Pflügers Arch.* **1981**, *391*, 85.
13. For a description of a $K_V1.3$ patch clamp assay, see: Grissmer, S.; Nguyen, A. N.; Aiyar, J.; Hanson, D. C.; Mather, R. J.; Gutman, G. A.; Karmilowicz, M. J.; Auperin, D. D.; Chandy, K. G. *Mol. Pharmacol.* **1994**, *45*, 1227; whole cell patch clamp recording was performed with $n \geqslant 2$ individual experiments at each compound concentration using different cells. Four or more different concentrations were determined per dose–response curve.
14. von Dobeneck, H.; Goltzsche, W. *Chem. Ber.* **1962**, *95*, 1484.
15. (a) Gilman, H.; Eisch, J.; Soddy, T. *J. Am. Chem. Soc.* **1957**, *79*, 1245; (b) Adam, W.; Groer, P.; Mielke, K.; Saha-Möller, C. R.; Hutterer, R.; Kiefer, W.; Nagel, V.; Schneider, F. W.; Ballmaier, D.; Schleger, Y.; Epe, B. *Photochem. Photobiol.* **1997**, *66*, 26.
16. (a) Curtin, D. Y.; Engelmann, J. H. *J. Org. Chem.* **1972**, *37*, 3439; (b) Leenders, R. G. G.; Scheeren, H. W. *Tetrahedron Lett.* **2000**, *41*, 9173.
17. Paterson, W.; Proctor, G. R. *J. Chem. Soc.* **1962**, 3468.
18. Compound effects on currents through IK-1 channels were tested in whole-cell patch clamp experiments according to Ref. 11 by comparison of the current amplitudes before and after compound application, with 1 mM 1-EBIO and 200 nM clotrimazole as controls for current activation and inhibition, respectively. Intracellular Ca^{2+} concentration was adjusted to 1 μM. Whole cell patch clamp recording was performed with $n \geqslant 2$ individual experiments at each compound concentration using different cells. Four or more different concentrations were determined per dose–response curve.
19. (a) Baell, J. B.; Gable, R. W.; Harvey, A. J.; Toovey, N.; Herzog, T.; Hänsel, W.; Wulff, H. *J. Med. Chem.* **2004**, *47*, 2326; (b) Harvey, A. J.; Baell, J. B.; Toovey, N.; Homerick, D.; Wulff, H. *J. Med. Chem.* **2006**, *49*, 1433; (c) Cianci, J.; Baell, J. B.; Flynn, B. L.; Gable, R. W.; Mould, J. A.; Paul, D.; Harvey, A. J. *Bioorg. Med. Chem. Lett.* **2008**, *18*, 2055. A general PBMC assay setup is described in (a), the readout was performed using BrdU Cell proliferation ELISA kit (Roche) according to manufacturer's instructions.
20. Thapsigargin-induced calcium increase: Fresh isolated PBMCs were stimulated for 48 h with 50 ng/mL anti-CD3 antibody (NatuTec). Non-adherent cells were harvested, suspended in 10^7 cells/mL concentration in culture medium (RPMI-1640, 10% FCS) and incubated with 3 μM Fluo3AM (Fischer Scientific), 0.1% Pluronic F-127 (Sigma–Aldrich) and anti-CD4-APC-antibody (BD Bioscience) for 30 min at rt. Cells were then washed twice with PBS, adjusted in culture medium to a final concentration of 5×10^5 cell/mL and incubated with the compounds or the corresponding amount of vehicle (DMSO) for 30 min. Intracellular calcium increase was induced with 25 μM thapsigargin (Sigma–Aldrich) and was measured using FACSCalibur (BD Bioscience). For the importance of calcium signaling in T-cell proliferation, see: (a) Vig, M.; Kinet, J.-P. *Nat. Immunol.* **2009**, *10*, 21; (b) Lewis, R. S. *Annu. Rev. Immunol.* **2001**, *19*, 497.
21. HaCaT keratinocytes were seeded in KBM/10% FCS and incubated for 24 h at 37 °C. Compounds were diluted in KBM/FCS with a final concn of 1% DMSO, added to the HaCaTs in triplicate and incubated for 48 h. For a readout on cell numbers, the Cell Titer Viability Assay from Promega was used.
22. Begenisich, T.; Nakamoto, T.; Ovitt, C. E.; Nehrke, K.; Brugnara, C.; Alper, S. L.; Melvin, J. E. *J. Biol. Chem.* **2004**, *279*, 47681.
23. Lang, F. *J. Am. Coll. Nutr.* **2007**, *26*, 613S.
24. Pegoraro, S.; Lang, M.; Feurle, J.; Kraus, J. U.S. Patent 7,276,606, 2005.
25. Chandy, K. G.; Wulff, H.; Beeton, C.; Pennington, M.; Gutman, G. A.; Cahalan, M. D. *Trends Pharmacol. Sci.* **2004**, *25*, 280.
26. Schmitz, A.; Sankaranarayanan, A.; Azam, P.; Schmidt-Lassen, K.; Homerick, D.; Hänsel, W.; Wulff, H. *Mol. Pharmacol.* **2005**, *68*, 1254.
27. Schmalhofer, W. A.; Bao, J.; McManus, O. B.; Green, B.; Matyskiela, M.; Wunderler, D.; Bugianesi, R. M.; Felix, J. P.; Hanner, M.; Linde-Arias, A.-R.; Ponte, C. G.; Velasco, L.; Koo, G.; Staruch, M. J.; Miao, S.; Parsons, W. H.; Rupprecht, K.; Slaughter, R. S.; Kaczorowski, G. J.; Garcia, M. L. *Biochemistry* **2002**, *41*, 7781.